



# Optimizing the Train-Catenary Electrical Interface Through Control Reconfiguration

António Martins<sup>1</sup>(✉), Vítor Morais<sup>1</sup>, Carlos Ramos<sup>1</sup>, Adriano Carvalho<sup>1</sup>,  
and João L. Afonso<sup>2</sup>

<sup>1</sup> Faculty of Engineering, University of Porto, Porto, Portugal  
{ajm,v.morais,cjr,asc}@fe.up.pt

<sup>2</sup> Centro ALGORITMI, University of Minho, Guimarães, Portugal  
jla@dei.uminho.pt

**Abstract.** Electric railway vehicles are supplied by substations and catenaries at increasingly high power levels being the interface between the traction motors and the overhead contact line based on power electronics converters. A large part of these are AC-DC four quadrant converters operating in parallel at relatively small switching frequencies but using the interleaving principle to reach a low harmonic distortion of the catenary current and imposing specific harmonic ranges in this current. However, the current is not a pure sinusoidal wave and its harmonics can excite unwanted resonances due to the combined effect of the catenary distributed parameters, the substation equivalent impedance and the current spectrum that can vary according to normal and abnormal operating conditions. This paper analyses this phenomenon and proposes a control strategy capable of minimizing the resonance effects.

**Keywords:** AC-DC converters · Electric railways · Interleaved converters · Resonance · Railway systems

## 1 Introduction

Across Europe, four major railway power supply systems exist: DC, with 1.5 kV and 3 kV voltage levels, and AC, with 50 Hz, 25 kV and 16.7 Hz, 15 kV. However, for mainlines, the most common supply is  $1 \times 25$  kV and  $2 \times 25$  kV, 50 Hz, and 15 kV, 16.7 Hz, [1]. Inside the traction vehicles one or more transformers, in case of AC supply, adapt the incoming high voltage to a lower one, more appropriate to feed the traction motors and the auxiliary equipment.

The interface between the intermediate DC-buses and the internal input AC voltage is made with different types of power electronics converters. These GTO or IGBT-based converters (single H-bridges, interleaved bridges or multilevel converters) operate under some kind of pulse-width modulation (PWM) method, are current-controlled ones and inject into the high-voltage catenary harmonics of different frequencies, magnitudes and time varying, [2–6]. These harmonics circulate in the catenary line and may originate network resonances. The resonance

voltages cause different problems such as overheating, interference with communication lines, operating errors in protection equipment and zero crossing-based systems, etc. High-frequency resonances occur frequently and can severely disrupt the normal railway operation, [7–9]. These resonances in the supply line have been analysed in different works, and most studies gave attention to the influencing factors of resonance occurrence, such as the length of conductors, [4], the position of trains [10], and the terminal impedances of power-quality conditioners, [11]. This paper is organised as follows: Sect. 2 presents the frequency response analysis of the catenary/substation impedance while Sect. 3 studies the behaviour of the four-quadrant converter while operating in inter-leaving mode. Section 4 presents the main simulation results in different operating conditions and the method to avoid resonances. Finally, Sect. 5 discusses the obtained results and concludes the paper.

## 2 Catenary Interface

The catenary interface using pulse-width modulated converters with nearly unity power factor is the most widely used solution in modern locomotives (e.g., electric multiple unit locomotives) because these converters easily provide bidirectional power flow, are modular and have a reduced harmonic content at the AC output. However, the analysis of the harmonic/resonance problem continues to be very important due to the wide range of frequencies of the injected voltages/currents.

### 2.1 Impedance Estimation

Several studies analyse the parallel and series resonances of the equivalent impedance at the traction system pantograph terminals, [4, 5, 11–15]. Knowledge of the harmonic impedance of catenary line is important for designing effective harmonic resonance mitigation measures. This knowledge is used in the design of harmonics filters inside the vehicles, the verification of harmonic limit requirements and the prediction of system resonance, [6, 13]. The frequency response of the catenary impedance can be, in some way, calculated using similar methods to those used in the estimation of the electric grid impedance.

A number of impedance measurement methods have been developed for this purpose: on-line and off-line methods, invasive or non-invasive, [16]. Although invasive methods give more accurate results (they achieve higher signal to noise ratio), in the context of catenary impedance estimation only on-line non-invasive methods should be considered. Nevertheless, the switching operation of PWM converters can also be considered an invasive method and thus a larger set of methods can be selected to estimate the catenary equivalent impedance. The complex impedance, in a specified range of frequencies, could be obtained by direct measurement of voltages and currents; frequency domain measurements constitute a direct means of measuring the frequency characteristics of system components. The measured voltages and currents can be used to calculate the equivalent impedance of the catenary and the connected converters at any

frequency but the measurement of this impedance function has proved inaccurate at those specific frequencies where parallel resonances occur. Here, the pantograph current reduces to very small values, owing to the high impedance of the line, [12]. Also the method is affected by non-linearities, saturation and noise. Alternatively, spectral analysis of time domain data of system operation can be used to determine the frequency domain characteristics, [17]. A second frequency method employs correlation power spectral density (PSD) analysis on the time domain voltage and current waveforms to obtain a transfer function, which approximates the catenary impedance as a function of frequency; a coherence coefficient is used to give a confidence level of the frequency response. The power spectral density describes the contribution of each frequency to the energy of the signal and the correlational analysis reduces the effect of noise and accounts for coupling between different frequencies due to non-linearities, [17]. In the identification of a catenary impedance model, the presence of an intermediate filter between the catenary and the on-board converters can be used in order to employ the same PSD approach, [12].

The application of other impedance identification methods, essentially employed in grid networks, like the extended Kalman filter, [18], the chirp z-transform, [19], and the so-called Resonance Mode Analysis, [20], can also be used in on-line conditions. In any case, knowledge of the system resonant frequencies is obtained and can be used to modify the switching frequency or the level of interleaving of the on-board converters, [21].

In terms of power electronics based solutions, different approaches have been employed in the past to reduce the harmonic distortion of the current injected into the catenary and thus avoiding major resonances, [2, 3, 22, 23]:

- Tuned harmonic filters, inserted between the pantograph and the high-voltage winding of the input transformer;
- Three-level converters instead of two-level converters on the catenary interface;
- Adaptive pulse width modulation for the feeding power converters;
- Installation of active filters or power quality conditioners.

None solution is completely effective but the use of the architecture and control flexibility of the interleaved two-level converters and three-level converters provides one the best starting approaches to deal with the issue, [3, 23, 24]. Additionally, the modularity of these two types of converters, namely the two-level ones, allows for a smooth degradation of operation in case of some types of failures, [21]. This paper focus its attention in the first ones. Thus, in order to optimize the performance of the converter sets in relation to their control, the interaction with other converters, and their performance in the supply system, it is important to determine the catenary impedance during the converter operation.

## 2.2 Catenary Model

The harmonic currents and voltages occurring along the catenary give rise to travelling waves of various frequencies, which are partly reflected at the electrical

line discontinuities caused by the presence of substations, [1]. The most common calculation method of the impedance seen by the pantograph consists in the replacement of a many wire catenary with a two wire transmission line, which is described by the well-known transmission line equations. Considering the simplified model in Fig. 1, the impedance of the left-side line section of length  $x$ ,  $Z_L$ , is given by (1), [2,4,25]:

$$Z_L = Z_0 \frac{Z_{tL} \cosh(\gamma x) + Z_0 \sinh(\gamma x)}{Z_0 \cosh(\gamma x) + Z_{tL} \sinh(\gamma x)} \quad (1)$$

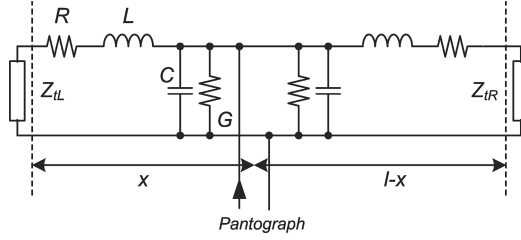


**Fig. 1.** Simplified model of the impedance seen by the train pantograph.

In Fig. 1,  $R$ ,  $L$ ,  $G$  and  $C$  correspond to series resistance and inductance, and parallel conductance and capacitance per unit length, respectively;  $Z_{tL}$  and  $Z_{tR}$  are the equivalent impedances of the left and right line section terminations, respectively. In (1),  $Z_0$ ,  $\gamma$  and  $\lambda$  define the characteristic impedance, propagation constant, and wave speed respectively. They are given by:

$$Z_0 = \sqrt{\frac{R + j\omega L}{G + j\omega C}} \quad (2)$$

$$\gamma = \sqrt{(R + j\omega L)(G + j\omega C)} \quad (3)$$

$$\lambda = \frac{1}{\sqrt{LC}} \quad (4)$$

The impedance of the right-side line section is obtained by substituting  $l - x$  for  $x$  in (1). In this set of parameters, the resistance  $R$  and the inductance  $L$  are frequency-dependent due to the skin effect in the soil underneath the railway track, while the capacitance  $C$  can be considered constant and eventually the conductance  $G$  can be neglected. The pantograph impedance is determined by the parallel of the two impedances: left and right sections, or

$$Z_P = Z_L // Z_R \quad (5)$$

In Fig. 2 is represented a simplified model of the contribution of one interleaved converter to the pantograph voltage.

Using the equivalent circuit in Fig. 2, the  $k^{th}$  harmonic voltage at the pantograph can be expressed in phasor notation as

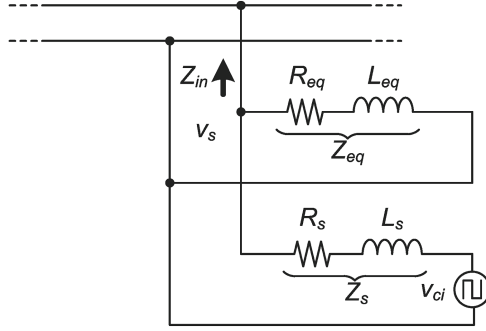


**Fig. 2.** Contribution of each converter voltage,  $v_{ci}$ , to the pantograph harmonics voltage.

$$V_{sk} = \sum_{i=1}^{N_T} V_{cik} \frac{Z_{pk}}{Z_{pk} + Z_{sk}} = V_{ck} \frac{Z_{pk}}{Z_{pk} + Z_{sk}} \quad (6)$$

where

$$X_{pk} = \frac{Z_{ink} Z_{eqk}}{Z_{ink} + Z_{eqk}} \quad (7)$$

and  $V_{sk}$  is the  $k^{th}$  harmonic root-mean-square (RMS) value of the pantograph voltage  $v_s$ ,  $V_{cik}$  is the  $k^{th}$  harmonic RMS value of the AC pulse voltage  $v_{ci}$ , and  $V_{ck}$  is the  $k^{th}$  harmonic RMS value of the composite AC pulse voltage  $v_c$  of the total converters.  $Z_{sk}$  is the  $k^{th}$  harmonic impedance of the leakage inductance and the internal resistance of the transformer,  $Z_{ink}$  is the input impedance seen from the pantograph, which can be quite difficult to estimate, as (1) and (5) clearly indicate. If the connection to the catenary includes some kind of filters the expression for the harmonics voltages  $V_{sk}$  becomes even more complex.

The resonant frequencies depend on the position of the vehicle, and are usually encountered between a few hundred Hz and several kHz, and above, depending on the circuit parameters. These frequencies are characterized by different damping coefficients which depend on: (i) the respective line distance, and (ii) the values of the electrical line parameters at the corresponding frequency. Typical parameters values of railway networks are presented in Table 1, [1, 8, 9, 15].

As an example, Fig. 3 shows the magnitude-frequency responses of the catenary impedance, estimated at different points, using  $R = 0.21 \Omega/\text{km}$ ,  $L = 1.2 \text{ mH}/\text{km}$ ,  $G = 0$ ,  $C = 11 \text{ nF}/\text{km}$   $L_{sub} = 2 \text{ mH}$ , and an open end at the other side;

**Table 1.** Typical parameters values of railway networks.

Structure	R, [ $\Omega/\text{km}$ ]	L, [ $\text{mH}/\text{km}$ ]	G, [ $\mu\text{S}/\text{km}$ ]	C, [ $\text{nF}/\text{km}$ ]
One track, one catenary	0.1 ... 0.3	1.2 ... 1.5	0.8 ... 1.0	11 ... 14
Two tracks, two catenaries	0.07 ... 0.1	0.75 ... 0.91	1.4 ... 1.8	18 ... 20

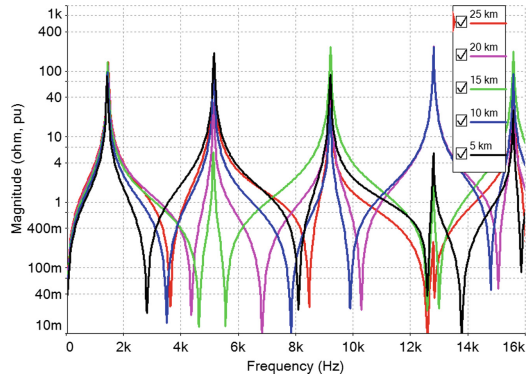


**Fig. 3.** Magnitude (in ohm, pu) of the impedance seen by the pantograph terminals as a function of the frequency and the distance of the train from the substation, with a section length of 30 km.

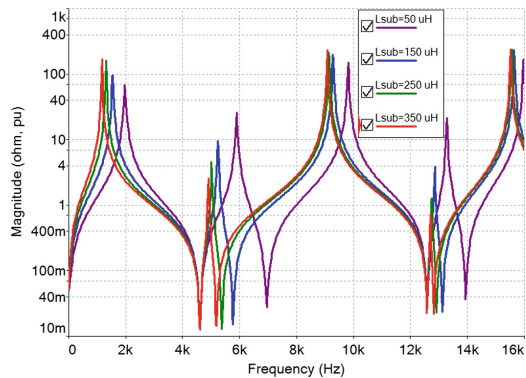


**Fig. 4.** Magnitude of the impedance seen by the pantograph terminals as a function of the substation impedance (in ohm, pu) with the train in the middle of a section with a length of 30 km.

parallel and series resonances are clearly exposed. The same parameters were used to evaluate the dependency of the catenary resonances according to the substation impedance and the results are shown in Fig. 4.

The low-frequency resonances are mainly affected by this uncertainty on the catenary and substation electrical parameters and, in order to assure a reliable operation, the relevant frequency ranges should be known. The harmonic excitation of the resonances is then suppressed if the specific frequencies, at which line resonances occur, are eliminated from the PWM spectrum. Of great importance is also the fact that in some frequency ranges the input admittance of the vehicle can exceed some critical negative real value so that the control may become unstable, [8, 9, 26, 27]. Thus, an appropriate control strategy for the PWM converter(s) must be based on a prior identification of the harmonic conditions in the overhead supply system or on a real-time knowledge of the same conditions.

### 3 Interleaved PWM Converters

The two-level four-quadrant converter is one of the best choices to supply the internal DC-link from the AC catenary, [2, 3, 23]. The presence of more than one converter is required to guarantee a high redundancy in case of failure and gives the opportunity to interleave them in order to reduce the harmonic content of the absorbed current, as represented in Fig. 5, [1–3, 21, 24, 28].

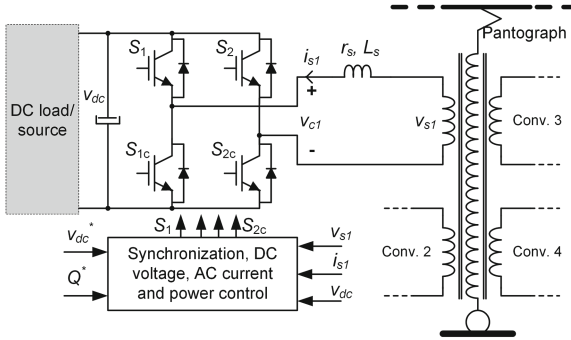


**Fig. 5.** Four interleaved four-quadrant converters and main control requirements.

Interleaving is achieved by phase shifting the carrier waveforms; for  $N$  converters the carrier shift will be  $\pi/N$ . The four-quadrant converter constitutes a voltage source that generates higher-order line voltage harmonics. The levels and frequencies of these harmonics depend on several factors, [23, 27]:

- The switching frequency,  $f_s$ , per converter phase leg;
- The number of interleaved bridges; the operation point of the vehicle (actual voltage and power);
- The power unbalance between independent systems, e.g., for each bogie;
- The modulation strategy in the converter control.

In general ideal conditions, the first main burst of harmonics are located as side-bands to the resultant frequency:

$$F_{res} = 2f_s N \quad (8)$$

It can be easily demonstrated that perfect harmonic cancellation will only occur if all the interleaved PWM converters are operating under ideal symmetrical conditions. This means that the following conditions must be simultaneously fulfilled:

- The converter bridges parameters are perfectly balanced;
- The interleaved PWM converter bridges have equal load sharing;
- The phase shift angle of the PWM converters is symmetrical.

The converters use closed loop controllers to regulate the DC-link voltage as well as the AC current. The goal of the control system strategy is to ensure unity power factor operation and DC-link voltage regulation; however, some amount of reactive power can eventually be used to stabilize the catenary voltage, [29]. An external DC voltage control loop using a PI controller maintains the DC-link voltage equal to its reference, when the load current or grid voltage vary, and an inner loop controls the AC input current using some kind of controller in order to control the power factor and current magnitude.

The control system requires several current and voltage sensors and, as a consequence, wrong or degraded measurements due to sensor or communication failures, seriously perturb the performance of the converter and may cause system malfunction. In the specific configuration and operation mode of two or more converters some additional common blocks are required: a current sharing module in order to equalize the power in each converter, and a phase synchronization block for optimizing the current spectrum in the primary side of the transformer, as shown in Fig. 6.

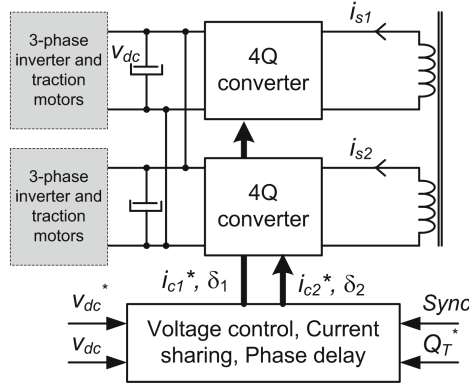


**Fig. 6.** Hierarchical control of the four-quadrant converters.  $v_{dc}^*$  is the reference voltage for the common DC-bus;  $i_{ci}^*$  is the total reference current for converter  $i$ ;  $\delta_i$  is the PWM phase for converter  $i$ ;  $Q_T^*$  is the reactive power reference.

Thus, a global control strategy for all PWM converters that eliminates the specific frequency bands from the harmonic spectrum of the pantograph should be devised in order to avoid the excitation of harmonic resonances under the actual conditions of the line. It involves the real-time identification of the resonance conditions (impedance), the estimation of the state of excitation of each actual resonant frequency and the generation of an appropriate switching strategy for the converters control. As more converters operate in interleaving mode and in balanced conditions, the equivalent harmonic voltages generated in the primary side of the transformer have lower magnitudes, higher frequencies and a wider spectrum. Thus, it is more difficult to excite resonances.

## 4 Simulation Results

A catenary with a length of 30 Km divided into 6 sections was used with the parameters  $R = 0.21 \Omega/\text{km}$ ,  $L = 1.2 \text{ mH}/\text{km}$ ,  $G = 0$ ,  $C = 11 \text{ nF}/\text{km}$   $L_{sub} = 2 \text{ mH}$ , and an open end at the other side. With these parameters the first resonant frequency is located between 1380 and 1400 Hz along the all catenary, as can be concluded from Fig. 3. The other relevant parameters used in the simulations are listed in Table 2. In order to achieve decoupled power control, a vector control approach was used for the AC current controller using the  $90^\circ$  phase delay for creating the beta component of the current.

**Table 2.** Parameters values used in the simulations.

Parameter	Value/Type
Substation nominal power	20 MVA
Substation impedance	$0.003 + i0.02 \text{ p.u.}$
Transformer voltage: pr./sec	25 kV/0.9 kV
Transformer impedance	$0.01 + i0.02 \text{ p.u.}$
DC-bus voltage	1.4 p.u.
Switching frequency	600 Hz
AC current controller	dq-axes, PI-type

The two relevant conditions related to the four-quadrant converters are exemplified in the next figures, where the train position is located 10 Km away from the open end. Figure 7 shows two secondary currents and the primary current (converter 1, which serves as phase reference, and converter 3, with a  $90^\circ$  shifted PWM carrier; converters 2 and 4 have carriers phase shifted by  $45^\circ$  and  $135^\circ$ , respectively) while Fig. 8 contains the spectrum of one secondary current and of the primary current. It is clearly demonstrated the harmonic cancellation occurring in the primary current.

### 4.1 Unbalanced Current

As referred before, two conditions negatively affect the harmonic cancellation in the primary current and thus the avoidance of resonances can be no longer possible: current unbalance and phase shift asymmetry. Figure 9 shows the result of a malfunction in the current balancing module: at  $t = 0.25 \text{ s}$ , converter 1 and 2 become not balanced (with  $I_{s1} = 1.3 \text{ p.u.}$  and  $I_{s2} = 0.7 \text{ p.u.}$ ) while converters 3 and 4 are still balanced; also shown is the primary current.

The steady-state catenary voltage is shown in Fig. 10 and its harmonic spectrum in Fig. 11; in the two figures, and due to the appearance of harmonics in the primary current centred at 1.2 kHz (twice the switching frequency) and multiples, a small excitation of the resonance mode can be noticed.

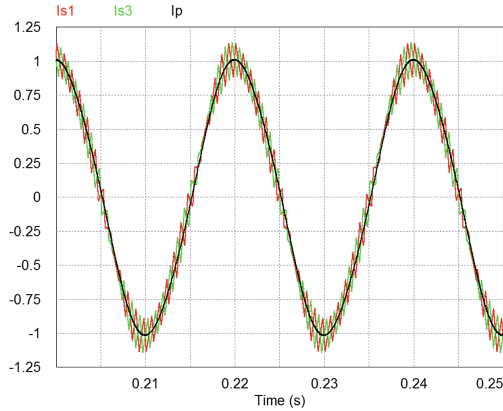


**Fig. 7.** Two secondary currents and the primary current in normal operation mode.

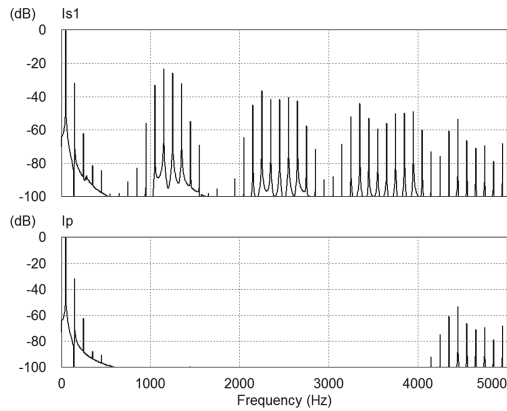


**Fig. 8.** Secondary and primary currents spectrum showing harmonic cancellation.

The steady-state catenary voltage is shown in Fig. 10 and its harmonic spectrum in Fig. 11; in the two figures, and due to the non-cancellation of harmonics in the primary current, components centred at multiples of 1.2 kHz (twice the switching frequency) have relevant magnitudes and a substantial excitation of the resonance mode is present (at around 1400 Hz, as referred above).

## 4.2 Loss of Synchronization

The potential occurrence of phase asymmetry is of more concern; harmonic cancellation is highly dependent on the fulfilment of this condition. Figure 12 shows the result of a loss of synchronization (starting at  $t = 0.3$  s) between converters 1 and 2: converter 1 and 2 have in-phase PWM signals while converters 3 and 4 still have the correct phase shift. As can be seen, currents  $I_{s1}$  and  $I_{s2}$  are in phase and the primary current is more distorted.

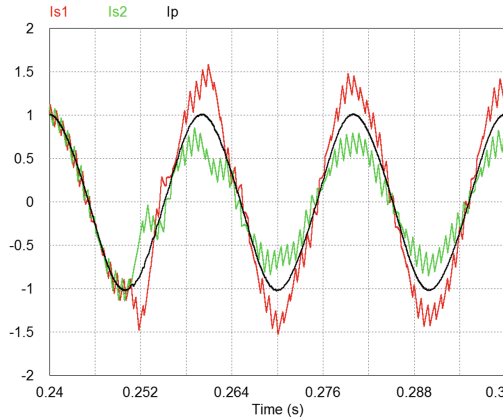


**Fig. 9.** Transient and steady-state current unbalance in converters 1 and 2.

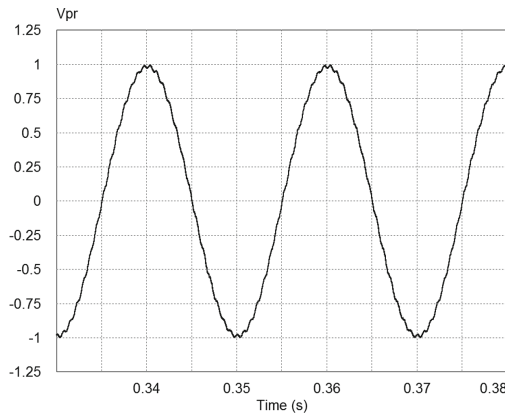


**Fig. 10.** Catenary voltage under current unbalance in the different converters.

The steady-state catenary voltage is shown in Fig. 13 and its harmonic spectrum in Fig. 14; in the two figures, and due to the non-cancellation of harmonics in the primary current, components centred at multiples of 1.2 kHz (twice the switching frequency) have relevant magnitudes and a substantial excitation of the first resonance mode is present (at around 1400 Hz, as referred above).

### 4.3 Proposed Method

The method proposed to avoid resonant conditions is based on the detection of the catenary resonant voltage made using fast Fourier transform analysis. When a resonant condition is detected the interleaved operation of the converters is lost and the current controller changes the PWM switching pattern in two ways: the switching frequency is changed to twice the normal value and there is no synchronization between any converter.

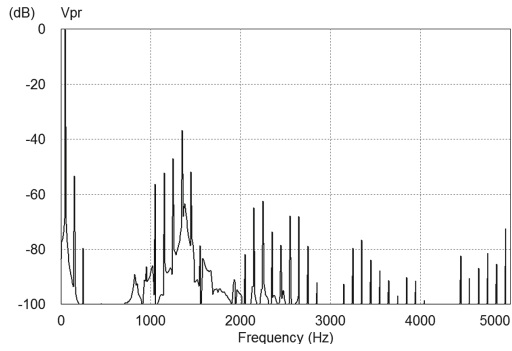


**Fig. 11.** Spectrum of the catenary voltage showing components around twice the switching frequency.

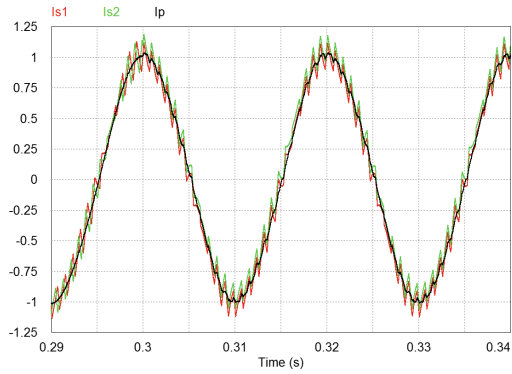


**Fig. 12.** Synchronization loss between converters 1 and 2, starting at  $t = 0.3$  s.

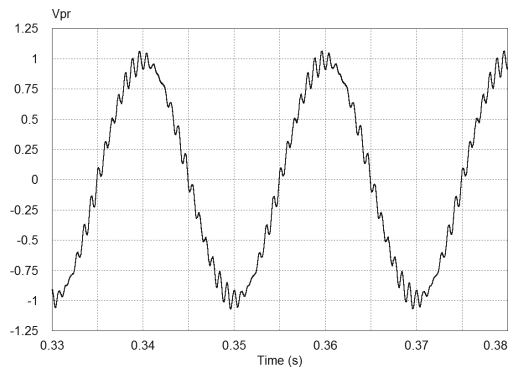


**Fig. 13.** Catenary voltage near resonance conditions.

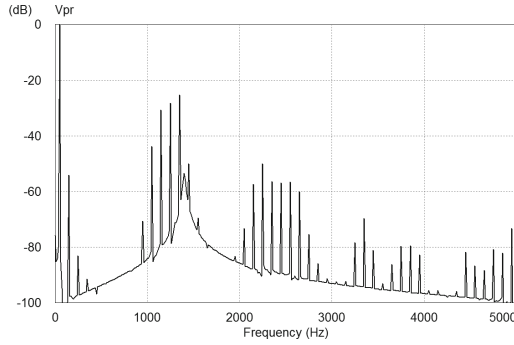


**Fig. 14.** Spectrum of the catenary voltage showing resonance conditions.

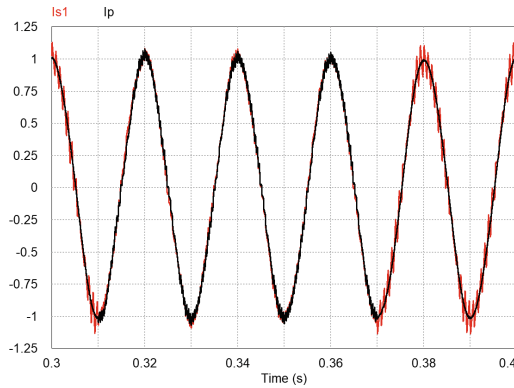


**Fig. 15.** One secondary current ( $I_{s1}$ ) and the primary current ( $I_p$ ) in normal operation and when a resonance condition is detected (between  $t = 0.31$  s and  $t = 0.37$  s).

This operation mode is a degraded one since the switching losses are increased and the catenary current is more distorted but the resonance condition is avoided. In Fig. 15 the resonance conditions occur between  $t = 0.31$  s and  $t = 0.37$  s. After being detected the switching frequency is changed to twice the nominal one in all converters with any type of synchronization. As can be seen, during loss of synchronism the converter current becomes more sinusoidal but the primary current increases its distortion. On the other hand, as shown in Fig. 16, the catenary voltage slightly increases its distortion during that time interval but only in a small magnitude as quantified in Fig. 17.

Comparing the catenary voltage either in time domain (Figs. 13 and 16) and in frequency domain (Figs. 14 and 17) it is clear the avoidance of the resonance conditions. The approach requires the detection of the resonance occurrence, e.g. using a total harmonic distortion measurement, and knowledge of the equivalent characteristic impedance seen by the pantograph terminal in order to change the switching frequency. That impedance is mainly dependent on the catenary/rail

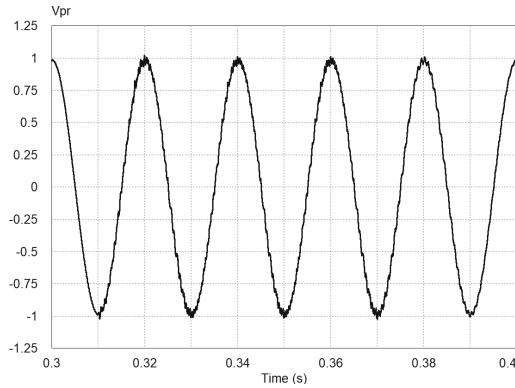


**Fig. 16.** Catenary voltage during loss of synchronism with different switching conditions (between  $t=0.31$  s and  $t=0.37$  s).

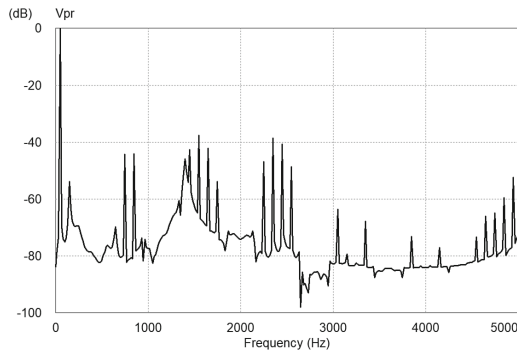


**Fig. 17.** Spectrum of the catenary voltage with different switching conditions.

distributed parameters and substation impedance and not on the train position or the number of trains in the track, as shown in Fig. 4 and also demonstrated in [2, 4, 7].

## 5 Conclusions

Modern electric traction systems employ four-quadrant converters operating in parallel with an interleaved switching strategy in order to achieve a very low current harmonic distortion. However, the existence of power unbalance between the converters or the loss of synchronism between the converters controllers originates resonance effects in the overhead contact line that can create high levels of harmonics voltages along the catenary. This paper presented a control reconfiguration approach capable of maintaining the converters operating in parallel without exciting relevant resonances.

**Acknowledgments.** The research has received funding from the FCT (Fundação para a Ciência e Tecnologia) under grant PD/BD/128051/2016. This work was partially supported by: FCT R&D Unit SYSTEC - POCI-01-0145-FEDER-006933/SYSTEC funded by FEDER funds through COMPETE 2020 and by national funds through the FCT/MEC, and co-funded by FEDER, in the scope of the PT2020 Partnership Agreement.

## References

1. Brenna, M., Foiadelli, F., Zaninelli, D.: *Electrical Railway Transportation Systems*, 1st edn. IEEE Press - Wiley, Hoboken (2018)
2. Holtz, J., Klein, H.-J.: The propagation of harmonic currents generated by inverter-fed locomotives in the distributed overhead supply system. *IEEE Trans. Power Electron.* **4**(2), 168–174 (1989)
3. Chang, G.W., Lin, H.-W., Chen, S.-K.: Modeling characteristics of harmonic currents generated by high-speed railway traction drive converters. *IEEE Trans. Power Deliv.* **19**(2), 766–773 (2004)
4. Zynovchenko, A., Xie, J., Jank, S., Klier, F.: Resonance phenomena and propagation of frequency converter harmonics in the catenary of railways with single-phase AC. In: *Proceedings of the EPE 2005*, 11–14 September, Dresden (2005)
5. Wang, B., Han, X., Gao, S., Huang, W., Jiang, X.: Harmonic power flow calculation for high-speed railway traction power supply system. In: Jia, L., Liu, Z., Qin, Y., Zhao, M., Diao, L. (eds.) *EITRT 2013*. LNEE, vol. 287, pp. 11–25. Springer, Heidelberg (2014). [https://doi.org/10.1007/978-3-642-53778-3\\_2](https://doi.org/10.1007/978-3-642-53778-3_2)
6. Hu, H., He, Z., Gao, S.: Passive filter design for China high-speed railway with considering harmonic resonance and characteristic harmonics. *IEEE Trans. Power Deliv.* **30**(1), 505–514 (2015)
7. Janssen, M.F.P., Gonçalves, P.G., Santo, R.P., Smulders, H.W.M.: Simulations and measurements on electrical resonances on the Portuguese 25 kV network. In: *Proceedings of the 8th World Congress on Railway Research, WCRR 2008*, 18–22 May, Seoul, Korea (2008)
8. Suarez, J.: *Étude et modélisation des interactions électriques entre les engins et les installations fixes de traction électrique 25 kV–50 Hz*. Ph.D. thesis, GEET-INP, Toulouse, France (2014)
9. Hu, H., Tao, H., Blaabjerg, F., Wang, X., He, Z., Gao, S.: Train-network interactions and stability evaluation in high-speed railways - part I: phenomena and modeling. *IEEE Trans. Power Electron.* **33**(6), 4627–4642 (2018)
10. Lee, H., Lee, C., Jang, G., Kwon, S.-H.: Harmonic analysis of the Korean high-speed railway using the eight-port representation model. *IEEE Trans. Power Deliv.* **21**(2), 979–986 (2006)
11. Brenna, M., Capasso, A., Falvo, M.C., Foiadelli, F., Lamedica, R., Zaninelli, D.: Investigation of resonance phenomena in high speed railway supply systems: theoretical and experimental analysis. *Electric Power Syst. Res.* **81**, 1915–1923 (2011)
12. Holtz, J., Krah, J.O.: On-line identification of the resonance conditions in the overhead supply line of electric railways. *Electr. Eng.* **74**(1), 99–106 (1990)
13. Mariscotti, A., Pozzobon, P.: Synthesis of line impedance expressions for railway traction systems. *IEEE Trans. Veh. Technol.* **52**(2), 420–430 (2003)
14. Dolara, A., Gualdoni, M., Leva, S.: Impact of high-voltage primary supply lines in the  $2 \times 25$  kV–50 Hz railway system on the equivalent impedance at pantograph terminals. *IEEE Trans. Power Deliv.* **27**(1), 164–175 (2012)

15. Monjo, L., Sainz, L.: Study of resonances in  $1 \times 25$  kV AC traction systems. *Electr. Power Compon. Syst.* **43**(15), 1771–1780 (2015)
16. Robert, A., Deflandre, T.: Guide for assessing the network harmonic impedance. In: *Proceedings of the 14th International Conference and Exhibition on Electricity and Distribution, CIRED 1997, 2–5 June (IEEE Conference Publication No. 438) (1997)*
17. Girgis, A., McManis, R.B.: Frequency domain techniques for modelling distribution or transmission networks using capacitor switching induced transients. *IEEE Trans. Power Deliv.* **4**(3), 1882–1890 (1989)
18. Hoffmann, N., Fuchs, F.W.: Minimal invasive equivalent grid impedance estimation in inductive-resistive power networks using extended Kalman filter. *IEEE Trans. Power Electron.* **29**(2), 164–175 (2014)
19. Duda, K., Borkowski, D., Bień, A.: Computation of the network harmonic impedance with chirp z-transform. *Metrol. Measur. Syst.* **16**(2), 299–312 (2009)
20. Xu, W., Huang, Z., Cui, Y., Wang, H.: Harmonic resonance mode analysis. *IEEE Trans. Power Deliv.* **20**(2), 1182–1190 (2005)
21. Perreault, D.J., Kassakian, J.G.: Distributed interleaving of paralleled power converters. *IEEE Trans. Circ. Syst.-I: Fundam. Theor. Appl.* **44**(8), 728–735 (1997)
22. Tan, P.-C., Loh, P.C., Holmes, D.G.: Optimal impedance termination of 25-kV electrified railway systems for improved power quality. *IEEE Trans. Power Deliv.* **20**(2), 1703–1710 (2005)
23. Zhang, R., Lin, F., Yang, Z., Cao, H., Liu, Y.: A harmonic resonance suppression strategy for a high-speed railway traction power supply system with a SHE-PWM four-quadrant converter based on active-set secondary optimization. *Energies* **10**, 1567–1589 (2017)
24. Holtz, J., Krah, J.O.: Suppression of time-varying resonances in the power supply line of AC locomotives by inverter control. *IEEE Trans. Ind. Electron.* **39**(3), 223–229 (1992)
25. Qiujiang, L., Mingli, W., Junki, Z., Kejian, S., Liran, W.: Resonant frequency identification based on harmonic injection measuring method for traction power supply systems. *IET Power Electron.* **11**(3), 585–592 (2018)
26. Sun, J.: Impedance-based stability criterion for grid-connected inverters. *IEEE Trans. Power Electron.* **26**(11), 3075–3078 (2011)
27. Cespedes, M., Sun, J.: Adaptive control of grid-connected inverters based on online grid impedance measurements. *IEEE Trans. Sustain. Energy* **5**(2), 516–523 (2014)
28. Youssef, A.B., El Khil, S.K., Slama-Belkhdja, I.: State observer-based sensor fault detection and isolation, and fault tolerant control of a single-phase PWM rectifier for electric railway traction. *IEEE Trans. Power Electron.* **28**(12), 5842–5853 (2013)
29. Bahrani, B., Rufer, A.: Optimization-based voltage support in traction networks using active line-side converters. *IEEE Trans. Power Electron.* **28**(2), 673–685 (2013)